Journal of Engineering Mathematics, Vol. 3, No. 1, January 1969
Wolters-Noordhoff Publishing – Groningen
Printed in the Netherlands

Calculation of Unsteady Flows Due to Small Motions of Cylinders in a Viscous Fluid

E. O. TUCK*

*California Institute of Technology***

(Received July 12, 1968)

SUMMARY
The problem of small oscillations of a cylinder of general cross-section in a viscous fluid is formulated in terms of integral equations. Numerical solutions of the integral equation are presented for the special case of a ribbon of zero thickness.

1. Introduction

The specific problem of interest concerns small sinusoidal vibrations of a ribbon of finite width $2a$, but negligible thickness, moving normal to itself in a viscous fluid, and the final result of this report is a numerical solution for the force components (added mass and damping coefficients) on the ribbon. Care is taken with the numerical solution to ensure a correct treatment of the singularity at the edges of the ribbon, and also to seek a result which is of uniform accuracy with respect to the frequency σ of oscillation. Results computed over a range of the parameter $\beta = \sigma a^2/\nu$ from 0.1 to 1000 indicate that the linearized forces on the ribbon differ little from those on a circular cylinder of diameter $2a$.

Although the above is the problem of most direct interest and was studied because of possible application to prediction of the effect of bilge keels on ships, a more general formulation is used to derive an integral equation, which is solved numerically only for the above special case. By use of Laplace transforms and a version of Green's theorem, the initial-value problem for arbitrary small motions of a deformable cylinder of arbitrary cross-section is reduced to solution of coupled integral equations, the unknowns being the pressure and vorticity distributions on the cross-section.

2. Unsteady Stokes Flow in Two Dimensions

In this paper we shall be concerned exclusively with the linearized Navier–Stokes equations, which describe unsteady Stokes flows. We shall in addition restrict attention to flows which are caused by the movement of cylindrical bodies. The surface of the cylinder, which need not in the general case be rigid, may move in any direction, but in order to justify linearization we must insist that those components of its velocity which are perpendicular to the cylinder axis are small in some sense.

It is not proposed at this time to investigate the degree of uniformity of the linearization process, or to attempt to find second-order solutions (e.g. steady "acoustic" streaming flows), interesting as such questions are. We shall accept that if A is some measure of the amplitude of the transverse motions of the cylinder, then as $A \to 0$ the exact solution of the Navier–Stokes equations tends almost everywhere to a solution of the Stokes equations. Although this is a reasonable viewpoint mathematically, it does of course limit severely the practical application of the results in cases (such as the ribbon oscillation in which we are most interested!) where we have reason to suspect that the amplitude A has to be extremely small in order to

* This work has been carried out under the support of the Office of Naval Research, Contract N0014-67-A-0094-0011.
** Present address: University of Adelaide, South Australia.

prevent non-linear convective effects (e.g. vortex generation at the edges) from becoming dominant.

If $\boldsymbol{u}=\boldsymbol{i}u(x, y, t)+\boldsymbol{j}v(x, y, t)+\boldsymbol{k}w(x, y, t)$ is the fluid velocity vector and $p(x, y, t)$ the pressure, the z or $\boldsymbol{k}$ direction being along the cylinder axis, then the linearized problem is specified by the equations

$$\frac{\partial \boldsymbol{u}}{\partial t} = -\frac{1}{\rho}\nabla p+\nu\nabla^2\boldsymbol{u}\,, \tag{2.1}$$

$$\nabla\cdot\boldsymbol{u}=0\,, \tag{2.2}$$

in the flow region exterior to a fixed curve C. This curve may be taken to define the equilibrium or average cross-section of the cylinder, as in Fig. 1. The boundary condition at infinity is that $\boldsymbol{u}\to 0$ in a sufficiently rapid manner, while on C we have

$$\boldsymbol{u}=\boldsymbol{U}(x, y, t)\,, \tag{2.3}$$

where $\boldsymbol{U}$ is a given velocity vector. For a rigid body in translation $\boldsymbol{U}=\boldsymbol{U}(t)$ only, but we may for the general discussion allow an arbitrary given time and space distribution of velocity on C,

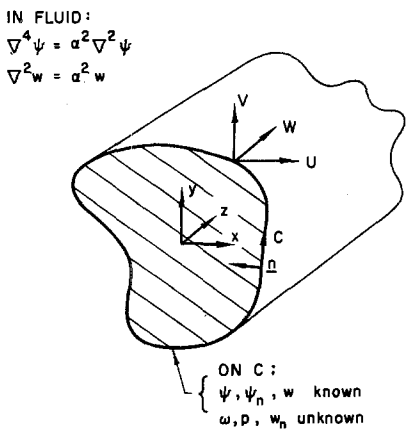

Figure 1. Sketch of the boundary-value problem for oscillating cylinders of arbitrary cross-section in a viscous fluid.

corresponding to a possible deforming cylinder. For simplicity, and indeed without loss of generality in the present linear model, we take our initial conditions to correspond to a state of rest.

The continuity equation (2.2) is as usual satisfied identically by introduction of a stream function $\psi(x, y, t)$ satisfying

$$u=\psi_y\,, \quad v=-\psi_x\,, \tag{2.4}$$

and if we set

$$\omega=v_x-u_y=-\nabla^2\psi\,, \tag{2.5}$$

the $\boldsymbol{k}$ component of the curl of (2.1) yields

$$\frac{\partial\omega}{\partial t} = \nu\nabla^2\omega\,, \tag{2.5}$$

while the $\boldsymbol{k}$ component of eq. (2.1) itself is

$$\frac{\partial w}{\partial t} = \nu\nabla^2 w\,. \tag{2.7}$$

Thus the motion w in the direction of the cylinder axis (which need not be small) is not coupl-

ed with the linearized motions in the cross-sections, but satisfies the same differential equation as the k-component ω of the vorticity.

Before applying Green's theorem to obtain formal solutions of these equations it is convenient to entirely remove the time dependence by taking Laplace transforms. For example,

$$w^*(x, y, s) = \mathscr{L}w(x, y, t) = \int_0^\infty w(x, y, t)\,e^{-st}\,dt \tag{2.8}$$

would define a new analytic function w^* of s, in the right-half s-plane. However, in the spirit of Heaviside we shall immediately abandon the star notation, using the same variable for a function and its $\mathscr{L}$-transform, the dependence on s rather than t indicating which is meant. The $\mathscr{L}$-transform of eq. (2.7) gives simply

$$\nabla^2 w = \alpha^2 w \tag{2.9}$$

where $\alpha^2 = s/\nu$, with an identical equation for ω. The equation satisfied by the stream function is then

$$\nabla^4 \psi = \alpha^2 \nabla^2 \psi\,. \tag{2.10}$$

In the following section we write down integral equivalents of these partial differential equations.

Taking the inverse transform once the solution for the transformed quantity has been found is a routine, if formidable, task using the inversion integral. However, since we are mainly interested in steady oscillations, we recall a standard result from linear systems analysis, that the amplitude of the ultimate response of a *stable* linear system to an input which is sinusoidal at radian frequency σ is obtained, in magnitude and phase, by setting $s = i\sigma$ in the Laplace transform. From this viewpoint, the Laplace transform variable s is merely a convenient symbol for $i\sigma$, with the advantage that we may avoid any convergence questions that might arise by allowing s to have a small *positive* real part throughout all but the final step in the analysis.

Before leaving this question it is well to point out that stability in the present context is sometimes only narrowly achieved. While viscosity provides dissipation, so that there can be no poles in the right-half s-plane, there is a kind of singular behavior at the origin $s=0$, as a result of Stokes' paradox. For as s or $\alpha \to 0$, (2.10) reduces to the biharmonic equation, which has no non-trivial solution bounded at infinity. An investigation such as that given in Appendix I indicates that the transfer function $\mathscr{L}$(force)/$\mathscr{L}$(velocity) behaves like $(\log s)^{-1}$ as $s \to 0$. Thus Stokes' paradox reveals itself if we observe that the velocity response to a step function force increases indefinitely, like $\mathscr{L}^{-1}(\log s/s) \sim \log t$. Conversely, the transient force required to set up an oscillation about a fixed point decays like $\mathscr{L}^{-1}(s/\log s) \sim t^{-2}(\log t)^{-3}$, while if the mean position of the cylinder moves through a finite distance the decay rate is like $t^{-1}(\log t)^{-2}$, and if it moves an infinite distance, only like $(\log t)^{-1}$.

3. Integral Representations

If $\Omega(x, y; x'y')$ is any solution of

$$\nabla^2 \Omega - \alpha^2 \Omega = \delta(x-x')\,\delta(y-y') \tag{3.1}$$

and $w(x, y)$ is any solution of (2.9), then by application of Green's theorem we have

$$w(x', y') = \int_C (w\Omega_n - w_n \Omega)\,dl\,, \tag{3.2}$$

where suffix n implies differentiation normal to the boundary C, out of the field of flow. Strictly the boundary of the flow should include a closing contour at infinity, but we rely on our boundary condition at infinity to eliminate contribution from that source. When w really does mean the z-component of velocity, which is given on C, eq. (3.2) provides us immediately with an integral equation to solve for the unknown stress w_n. This equation has been discussed by Levine (1957) and others, for several choices of C and Ω.

Since ω and w satisfy the differential equation, (3.2) also applies when ω is substituted for w throughout. However, now *both* ω and ω_n are unknown on C; what we really need is an integral representation of the equation (2.10) for ψ. We establish this representation in a rather oblique manner, with physical significance. On taking the divergence of (2.1) we obtain the well-known result that the pressure p is harmonic, i.e. $\nabla^2 p = 0$. Define $q(x, y)$ to be the harmonic conjugate of p, satisfying the Cauchy–Riemann equations $p_x = q_y$, $p_y = -q_x$. By inspection of (2.1) after $\mathscr{L}$-transformation, it is easy to see that these equations are satisfied if we choose

$$q = -\mu(\omega + \alpha^2 \psi)\,. \tag{3.3}$$

Since $\nabla^2 q = 0$, we can use any Green's function $G(x, y; x', y')$ for Laplace's equation, satisfying $\nabla^2 G = \delta$, to obtain

$$q = \int_C (qG_n - q_n G)\,dl\,. \tag{3.4}$$

Substituting (3.3) in (3.4) and using (3.2) to eliminate ω from the lefthand side, we have

$$\psi = \int_C [(\psi G_n - \psi_n G) - (\omega \Psi_n - \omega_n \Psi)]\,dl\,, \tag{3.5}$$

where

$$\Psi = -\frac{1}{\alpha^2}(\Omega - G) \tag{3.6}$$

is the Green's function for eq. (2.10), i.e. satisfies $\nabla^4 \Psi - \alpha^2 \nabla^2 \Psi = \delta$.

Equation (3.5) is essentially the Green's theorem for the partial differential equation (2.10), and indicates how ψ is known in the flow region if all four quantities ψ, ψ_n, $\omega = -\nabla^2 \psi$, $\omega_n = -\nabla^2 \psi_n$ are known on C. Since ψ and ψ_n are known (or readily obtainable from U) but ω, ω_n are not known on C, we need two equations to determine ω, ω_n. These are the result of applying on C successively (3.5) itself and the derivative of (3.5) normal to C, leading to a pair of coupled integral equations to determine ω, ω_n. It is somewhat more convenient to replace the unknown ω_n by an equivalent unknown p, setting

$$\begin{aligned} \omega_n &= -\alpha^2 \psi_n - \frac{1}{\mu} q_n \\ &= -\alpha^2 \psi_n - \frac{1}{\mu} p_l\,, \end{aligned} \tag{3.7}$$

where $p_l = \partial p/\partial l = \partial q/\partial n$ is the tangential derivative of the pressure along C. On substitution of (3.7) in (3.5) and integration by parts, the integrated part vanishes if we assume continuous pressure on C, leaving

$$\psi = \int_C \left[\psi G_n - \psi_n \Omega - \omega \Psi_n + \frac{1}{\mu} p \Psi_l\right] dl\,. \tag{3.8}$$

In this form of the Green's theorem, the basic unknowns are explicitly exhibited as the vorticity ω and pressure p on the surface. This is especially convenient for calculation of the forces on the cylinder, as we shall observe in the following section.

These integral formulations are of course useless for the purpose of obtaining numerical solutions, if we are unable to find and compute the Green's functions involved. We should like to force the Green's functions to satisfy boundary conditions on C, since this would eliminate some terms from the integral equations, but in the general case this is impossible. Thus we must fall back on Green's functions which are defined as analytic *everywhere* in the x, y plane except at $x = x'$, $y = y'$. These are functions of $R = \{(x - x')^2 + (y - y')^2\}^{\frac{1}{2}}$ only, and may be found and computed without trouble, the formulae being

$$G = \frac{1}{2\pi} \log R \tag{3.9}$$

$$\Omega = -\frac{1}{2\pi} K_0(\alpha R) \tag{3.10}$$

$$\Psi = -\frac{1}{2\pi\alpha^2} (\log R + K_0(\alpha R)) \tag{3.11}$$

where K_0 is the modified Bessel function of the third kind, zero order. It should be noted that G and Ω are logarithmically singular at $R=0$ but $\Psi = O(R^2 \log R)$, and that G and Ψ are logarithmically singular at infinity but Ω is exponentially small.

4. The Forces and Moment on the Cylinder

The vector force $\boldsymbol{F}$ and moment $\boldsymbol{M}$ about the origin on any three-dimensional body with surface S, moving in any manner whatsoever in an incompressible viscous fluid which is at rest at infinity, are given exactly by

$$\boldsymbol{F} = \int_S [-p d\boldsymbol{S} + \mu \boldsymbol{\omega} \times d\boldsymbol{S}], \tag{4.1}$$

$$\boldsymbol{M} = \int_S [\boldsymbol{r} \times (-p d\boldsymbol{S} + \mu \boldsymbol{\omega} \times d\boldsymbol{S}) + 2\mu \boldsymbol{u} \times d\boldsymbol{S}]. \tag{4.2}$$

The merit of these formulae (which can be obtained readily from the corresponding formulae involving the stress tensor) is that they are written directly in terms of the basic unknowns of pressure p and vorticity ω on the body surface. Any method, numerical or otherwise, which provides p and ω as primary output, also gives by quadrature the forces and moments, without recourse to calculation of the components of the stress tensor.

For the special case when S is the surface of a cylinder with cross-section C, eq. (4.1) has a z-component which merely gives the expected skin friction per unit length of cylinder,

$$\begin{aligned} F_z = \boldsymbol{k} \cdot \boldsymbol{F} &= \mu \int_C [w_x dy - w_y dx] \\ &= \mu \int_C w_n dl . \end{aligned} \tag{4.3}$$

The force components per unit length in transverse directions are

$$F_x = \boldsymbol{i} \cdot \boldsymbol{F} = \int_C [-p dy + \mu \omega dx], \tag{4.4}$$

$$F_y = \boldsymbol{j} \cdot \boldsymbol{F} = \int_C [p dx + \mu \omega dy], \tag{4.5}$$

and the moment per unit length about the cylinder axis is

$$M_z = \boldsymbol{k} \cdot \boldsymbol{M} = \int_C [p(x dx + y dy) + \mu\omega(x dy - y dx) - 2\mu(U dx + V dy)]. \tag{4.6}$$

It is interesting to observe that by re-introducing q from eq. (3.3) and defining the complex quantities $\zeta = x + iy$, $f(\zeta) = p + iq$, eqs. (4.4) and (4.5) may be combined to give

$$F_x + iF_y = -\rho s \int_C \psi d\zeta + i \int_C f(\zeta) d\zeta . \tag{4.7}$$

The first integral in (4.7) is known, while the second can be evaluated using the calculus of residues once we establish the analytic behavior of the function $f(\zeta)$, e.g. as $\zeta \to \infty$. However, we shall make no use of eq. (4.7).

Equations (4.4) and (4.5) give the forces on the cylinder directly in terms of the primary unknowns of the problem. From these forces, quantities which may be called added mass and damping coefficients may be obtained as in the following example. Suppose the cylinder pos-

sesses geometrical symmetry about the y-axis, and oscillates sinusoidally as a rigid body along the y-axis, with $v = V(t) = V_0 e^{i\sigma t}$. Then if the steady-state force response calculated from (4.5) is written as

$$F_y(t) = -(k - ik')\rho\pi a^2 i\sigma V_0 e^{i\sigma t}, \tag{4.8}$$

where $2a$ is the length of intercept of the cylinder section on the x-axis, then the coefficient k is the ratio between the added (or "virtual") mass of the cylinder and the displaced mass $\rho\pi a^2$ per unit length of a circular cylinder of radius a. Similarly k' may be interpreted as a damping coefficient, the component of force in phase with the velocity, per unit velocity, being

$$-\rho\pi a^2 \sigma k' = \mathscr{R}(F_y / V_0 e^{i\sigma t}). \tag{4.9}$$

For example, in 1851 Stokes (see Rosenhead 1963, p. 390) gave the following formula for k, k' as functions of non-dimensional frequency $\beta = \sigma a^2/\nu$, in the case when C is a circle:

$$k - ik' = 1 - \frac{4K_1(\sqrt{i\beta})}{\sqrt{i\beta}\, K_0(\sqrt{i\beta})}, \tag{4.10}$$

K_0, K_1 being modified Bessel functions of the third kind. Values of k, k' calculated from (4.10) are shown in Fig. 7.

5. Zero Thickness Ribbons

The integral representation (3.8) applies when C is any closed curve in the (x, y) plane. Consider now the special case $C = C_- + C_+$ where C_-, C_+ are the "bottom" and "top" sides of a cut in the plane as in Fig. 2. This cut represents a ribbon of zero thickness, and will be supposed to move

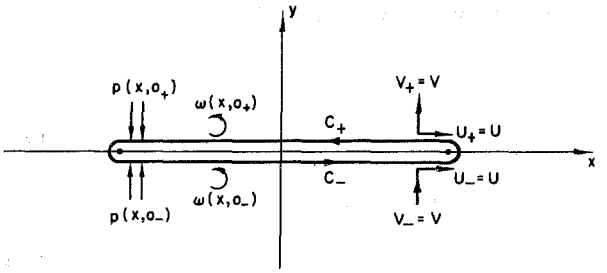

Figure 2. The boundary-value problem for a straight ribbon of negligible thickness.

without relative motion of its top and bottom faces. That is, we shall require continuity of ψ and ψ_n across the cut. Then (3.8) reduces to

$$\psi = \int_{C_-} \left[\Delta\omega \Psi_n - \frac{1}{\mu} \Delta p \Psi_l \right] dl \tag{5.1}$$

where $\Delta\omega$, Δp are the jumps in vorticity and pressure across the cut, e.g. $\Delta\omega = \omega|_{C_+} - \omega|_{C_-}$. Equation (5.1) does not appear to be a great simplification relative to (3.8), since the only portion of (3.8) eliminated involved terms which were in any case known.

However, in the special case illustrated by Fig. 2 of a ribbon whose equilibrium configuration is a straight segment, a substantial simplification can be made. Without loss of generality the ribbon can be taken to extend from $(-a, 0)$ to $(a, 0)$, in which case $dl = dx$, $\partial/\partial n = \partial/\partial y$ on C_-. Then (5.1) states that

$$\psi(x', y') = \int_{-a}^{a} \left[\Delta\omega(x) \Psi_y(x, 0; x', y') - \frac{1}{\mu} \Delta p(x) \Psi_x(x, 0; x', y') \right] dx .$$

But if we now apply this equation on $y' = 0$, and use the formula (3.11) for Ψ, which implies $\Psi_y(x, 0; x', 0) = 0$, we find

$$\psi(x', 0) = -\frac{1}{\mu}\int_{-a}^{a} \Delta p(x)\, \Psi_x(x, 0; x', 0)\, dx\,. \tag{5.3}$$

Similarly, on setting $y' = 0$ after differentiating (5.2) with respect to y', we have

$$U(x') = \psi_{y'}(x', 0) = \int_{-a}^{a} \Delta\omega(x)\, \Psi_{yy'}(x, 0; x', 0)\, dx\,. \tag{5.4}$$

Thus the normal and tangential oscillations of the ribbon are described by separate, uncoupled, integral equations (5.3) and (5.4) respectively. Normal motion V leads to a pressure jump Δp which is a solution of (5.3), but no jump in vorticity across the ribbon, while tangential motion U gives a vorticity jump $\Delta\omega$ but a continuous pressure. These conclusions could no doubt be obtained by purely physical arguments.

In the subsequent analysis we shall be concerned with normal motion, and thus with solutions of eq. (5.3). On differentiation with respect to x' we obtain

$$V(x') = -\psi_{x'}(x', 0) = \frac{1}{\mu}\int_{-a}^{a} \Delta p(x) \Psi_{xx'}(x, 0; x', 0)\, dx\,, \tag{5.5}$$

which is an integral equation of the form

$$\int_{-a}^{a} \Delta p(x) L(\alpha|x - x'|)\, dx = \mu V(x')\,, \tag{5.6}$$

where the kernel function $L = \Psi_{xx'}$ is obtainable from the formula (3.11) for Ψ,

$$L(z) = \frac{1}{2\pi}\frac{d^2}{dz^2}(\log z + K_0(z))\,. \tag{5.7}$$

For small values of its argument the kernel function has a logarithmic singularity, with an expansion of the form:

$$L(z) = -\frac{1}{4\pi}(\log z + \gamma + \tfrac{1}{2} - \log 2) + O(z^2 \log z)\,, \tag{5.8}$$

while for large $|z|$ we have

$$L(z) = -\frac{1}{2\pi z^2} + \frac{1}{\sqrt{8\pi z}}\, e^{-z}\left[1 + O\left(\frac{1}{z}\right)\right]\,. \tag{5.9}$$

Although it is possible (with care) to differentiate eq. (5.6) once more under the integral sign in order to obtain a singular integral equation with a Cauchy kernel, for which there exists a large body of general theory (e.g. Muskhelishvili (1953)), we prefer to attack eq. (5.6) itself by direct numerical methods. However, we observe in passing a result from the theory of singular integral equations, namely that unless $V(x)$ satisfies at least one very special side condition, any solution $\Delta p(x)$ is necessarily unbounded at the ends $x = \pm a$, and indeed possesses an inverse square root singularity at each end.

6. Numerical Solution for Steady Normal Oscillations

If we set $s = i\sigma$, $\alpha = \sqrt{i\sigma/\nu}$, in eq. (5.6) we can interpret this equation as a relationship between complex amplitudes in a steady sinusoidal oscillation. That is, after transients have decayed, the pressure jump due to $V(x)\, e^{i\sigma t}$ is $\Delta p(x)\, e^{i\sigma t}$, where V and Δp are related by (5.6). The particular case of greatest interest here, and the only case for which we shall present calculations, corresponds to rigid translatory oscillations, $V(x) = V_0 = \text{constant}$. It is convenient to define a non-dimensional co-ordinate $\xi = x/a$, pressure jump $P(\xi) = (a/\mu V_0)\Delta p(x)$, and frequency $\beta = \sigma a^2/\nu$. Then for the oscillation described above, eq. (5.6) becomes

$$\int_{-1}^{1} P(\xi)\, L(\sqrt{i\beta}|\xi - \xi'|)\, d\xi = 1\,. \tag{6.1}$$

The method we use to solve (6.1) numerically is quite direct, and consists simply of replacing

integration by summation, using a suitable quadrature formula. The integral equation now becomes a matrix-vector equation, which we solve by explicit inversion of the kernel matrix. The only sophistication in the numerical analysis comes in the decision as to which is a "suitable" quadrature formula. In spite of the arguments presented below, if we wished to achieve greatest economy in computer time a good case could be made for using the crudest possible method, e.g. the trapezoidal rule with equal intervals. Equal interval methods with a difference kernel have the advantage that if N intervals are used, only $2N$ evaluations of the kernel function are needed rather than N^2, and the trapezoidal rule has the advantage of equal weights, which eliminates at least $2N$ multiplications. However, since it was not expected that computer time would be a major problem*, the method used here is a little more sophisticated.

Three matters which might be cause for concern are (i) the logarithmic singularity of the kernel at $\xi=\xi'$, (ii) the square root singularities of $P(\xi)$ at $\xi=\pm 1$ and (iii) the fact that if β is large, the kernel contains a term (see (5.9)) which oscillates rapidly while decaying to zero. In fact a brute force method which simply pays no heed to the integrable singularities described in (i) and (ii) above is almost bound to work (see e.g. Davis and Rabinowitz 1965) albeit with some sacrifice in accuracy for a given N. As far as the logarithmic singularity is concerned, we should be thankful for its existence and make no attempt to "eliminate" it, even if this were possible, for this singularity of the kernel function makes the resulting kernel matrix diagonally dominant, and hence docile in its inversion properties. The square root singularities can be removed by changing variable from ξ to θ, where $\xi=\sin\theta$, say, or equivalently by using an unequal interval quadrature formula, with a square root bias towards the ends. For instance, if we use a dissection of the form $\xi=\xi_j=-\cos \pi j/N$, $j=0, \ldots, N$, this accomplishes exactly the same purpose as if we used an equal interval method in conjunction with the change of variable to θ.

The objection (iii) above concerning rapid oscillations of the integrand could of course be overcome by allowing N to increase with β, but since computer time increases like N^3 more efficient procedures are desirable. The method we use is to observe that we have no reason to expect the unknown $P(\xi)$ to vary rapidly (an expectation confirmed by the solution itself) and therefore approximate $P(\xi)$ but not the kernel L in our quadrature formula. Thus if we approximate that $P(\xi)=P_j=$ constant on each segment $\xi_j<\xi<\xi_{j+1}$, we have from (6.1)

$$\sum_{j=0}^{N-1} P_j \int_{\xi_j}^{\xi_{j+1}} L(\sqrt{i\beta}\,|\xi-\xi'|)\,d\xi = 1\,. \tag{6.2}$$

We now force this equation to hold at the mid-point $\xi=\xi'_k=\frac{1}{2}\xi_k+\frac{1}{2}\xi_{k+1}$ of the k'th segment, leading to a matrix equation of the form

$$\sum_{j=0}^{N-1} P_j A_{kj}=1\,, \qquad k=0, 1, \ldots, N-1 \tag{6.3}$$

where

$$A_{kj} = \int_{\xi_j}^{\xi_{j+1}} L(\sqrt{i\beta}\,|\xi-\xi'_k|)\,d\xi\,. \tag{6.4}$$

Of course if we now had to resort to further numerical quadrature to evaluate these matrix elements A_{kj}, we should have gained nothing, for the same objection would apply to the new quadrature, for large β. Fortunately the integration in (6.4) can be performed analytically and exactly, since the kernel $L(z)$ is already defined in (5.7) as the derivative of another function. Thus we can observe that

$$\begin{aligned} L(\sqrt{i\beta}\,|\xi-\xi'|) &= \frac{\partial}{\partial\xi}\,\frac{\operatorname{sgn}(\xi-\xi')}{\sqrt{i\beta}\cdot 2\pi\sqrt{i}}\left\{\frac{1}{\sqrt{\beta}\,|\xi-\xi'|}+\sqrt{i}K'_0(\sqrt{i}\sqrt{\beta}\,|\xi-\xi'|)\right\} \\ &= \frac{\partial}{\partial\xi}\,\frac{1}{2\pi i\sqrt{\beta}}\,F(\sqrt{\beta}(\xi-\xi')) \end{aligned} \tag{6.5}$$

* The program in fact requires about one minute of I.B.M. 7094 time per frequency, for the finest dissection used, $N=49$.

where

$$F(z) = \frac{1}{z} + ker'(z) + ikei'(z), \qquad z > 0, \tag{6.6}$$

and $F(-z) = -F(z)$. The functions *ker'*, *kei'* are Kelvin functions (Abramowitz and Stegun, 1964, p. 379), for which fast and accurate off-the-self computing procedures are available. Hence we have finally for the matrix element,

$$A_{kj} = \frac{1}{2\pi i\sqrt{\beta}} [F(\sqrt{\beta}(\xi_{j+1} - \xi'_k)) - F(\sqrt{\beta}(\xi_j - \xi'_k))], \tag{6.7}$$

a formula which allows setting up the matrix $[A_{kj}]$ with just N^2 calls upon the subroutine for the function F, no more than would be required for any other quadrature formula with unequal intervals. It should be observed in passing that the above method, while especially designed to provide uniform accuracy as β increases, has at the same time eliminated any problems with the logarithmic singularity of the kernel, for we have integrated straight through it in the analytic evaluation of the diagonal elements A_{kk}.

The immediate output from solution of the matrix equation (6.3) by inversion of $[A_{kj}]$ is the complex pressure jump function $P(\xi)$. Using this we obtain from (4.5) the force on the ribbon,

$$\begin{aligned} F_y &= -\int_{-a}^{a} \Delta p(x)dx \\ &= -\frac{\mu V_0}{a}\int_{-1}^{1} P(\xi)d\xi . \end{aligned} \tag{6.8}$$

The integral in (6.8) may be evaluated as the simple sum

$$\int_{-1}^{1} P(\xi)d\xi \sim \sum_j P_j(\xi_{j+1} - \xi_j),$$

since the bias in the interval lengths automatically takes care of the square root singularity in $P(\xi)$. From the real and imaginary parts of the complex force we can extract the damping coefficient and added mass respectively, as in eqs. (4.8), (4.9).

It is also interesting and easy to compute flow quantities in the fluid, on or off the ribbon. In particular the vertical component of velocity on the real axis is readily obtained from (5.5), and we have

$$v(a\xi, 0)/V_0 = \int_{-1}^{1} P(\xi) L(\sqrt{i\beta}|\xi - \xi'|)d\xi . \tag{6.9}$$

For $|\xi'| < 1$ this is just a re-statement of the integral equation (6.1), and can be used to provide a check, since we should find $v = V_0$. Values were actually computed from (6.9) for $\xi' = 0.95$ through 1.33.

A small amount of numerical experimentation was performed to find an adequate value of N. The somewhat arbitrary upper limit imposed by the available complex matrix inversion routine was $N = 50$, and values of 21, 31 and 49 were actually used. $N = 21$ seemed already to be very accurate except at the highest frequencies. For instance at $\beta = 1.0$ the change in the force components in going from $N = 21$ to $N = 31$ was only in the 6th significant figure, while at $\beta = 100.0$ this change had reached the 4th significant figure. At $\beta = 1000.0$ the values obtained for the force at $N = 21, 31, 49$ were proportional to $3.47 + i34.91$, $3.29 + i35.07$, $3.20 + i35.10$ respectively. The accuracy of the $N = 49$ result appears to be better than ± 0.1 in both real and imaginary parts, which represents a more serious relative error in the real (dissipative) part than in the larger imaginary part. In spite of the uniformizing procedure adopted, it would appear that we are at $\beta = 1000.0$ coming close to the upper limit of frequency for which acceptable accuracy could be attained; without this procedure we could probably not have even gone this far.

7. Computed Results

The pressure jump across the ribbon, primary output from the computer program, is shown in Figs. 3–5. Figure 3 gives the imaginary part of $P(\xi)$, i.e. the component of pressure jump in phase with the acceleration of the ribbon, for the lower frequencies $\beta = 0.1 - 1.0$. Also shown as a dashed curve is the asymptotic solution (A1.4) as $\beta \to 0$, with the constant C_2 chosen according to (A1.5) at $\beta = 0.1$. The agreement between the computed and asymptotic solutions is already good at $\beta = 0.1$. As β increases, the curvature of the pressure plot near the center of the plate decreases, and already at $\beta = 1.0$ the curve has become slightly concave downwards.

In Fig. 4, which is a continuation of Fig. 3 to higher frequencies $\beta = 10.0$–1000.0, we have plotted $\mathscr{I}P/\beta$ instead of $\mathscr{I}P$, in order to demonstrate the progression of the computed results towards the asymptotic solution (A1.9), shown dashed. The result at $\beta = 1000.0$ is already quite close to the asymptotic limit, but notice that this limit is non-uniform near the end $\xi = 1.0$, and the curve for $\beta = 1000.0$ turns up rapidly towards its required square-root singularity. This rapid break-away is of course the reason for the ultimate loss in accuracy of the numerical solution, discussed in the previous section, for even with a square root bias, we eventually lack a sufficient density of intervals near $\xi = 1.0$. The component $\mathscr{R}P$ in phase with the velocity is shown in Fig. 5, scaled with respect to $\sqrt{\beta}$, because we expect the asymptotic behavior as $\beta \to \infty$ to be $O(\sqrt{\beta})$.

In Fig. 6 we present the real part of the computed velocity component $v(a\xi, 0)$ on the x-axis in the fluid. For $\xi < 1$ we should find $v = V_0$, and any departure from this value must be interpreted as numerical error. In fact, except for $\beta = 1000.0$ the departure from $v = V_0$, is too small to see, in the scale of the figure. The result shown for $\beta = 1000.0$ exhibits a slight "smoothing-off" of the right-angle bend in the curve at $\xi = 1.0$, the extent of the smoothing depending on the number N of elements used, here $N = 49$. As ξ increases above 1.0, $\mathscr{R}v$ decreases from V_0,

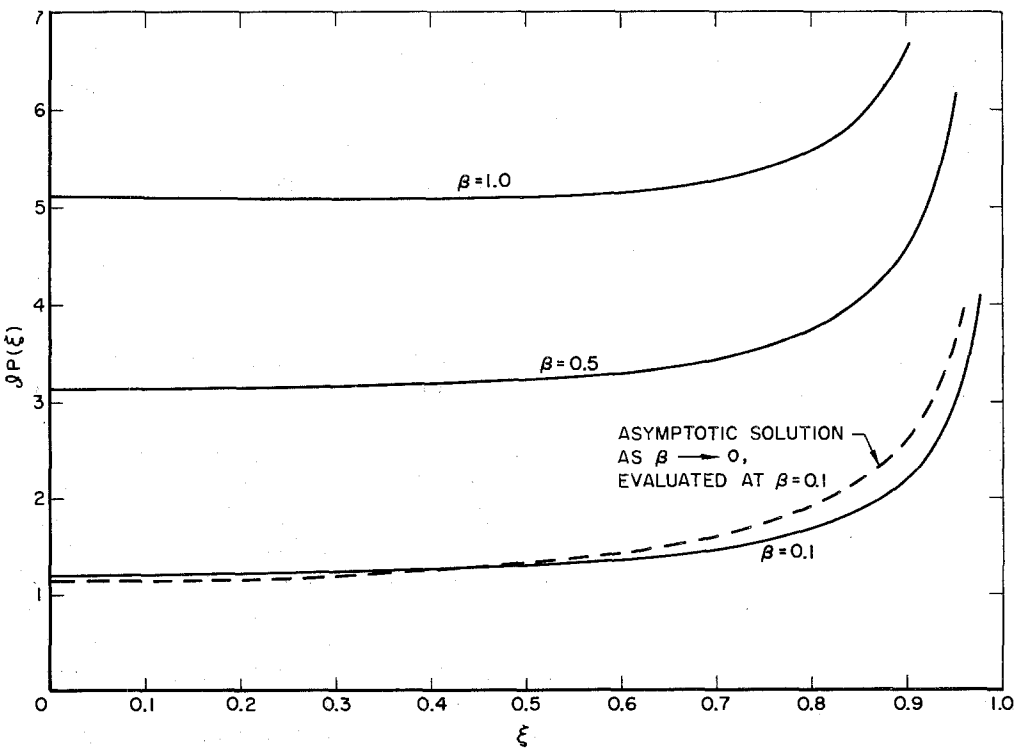

Figure 3. Pressure jump $\mathscr{I}P(\xi)$ across the ribbon in phase with acceleration. Computations for low frequencies $\beta = 0.1$ to $\beta = 1.0$.

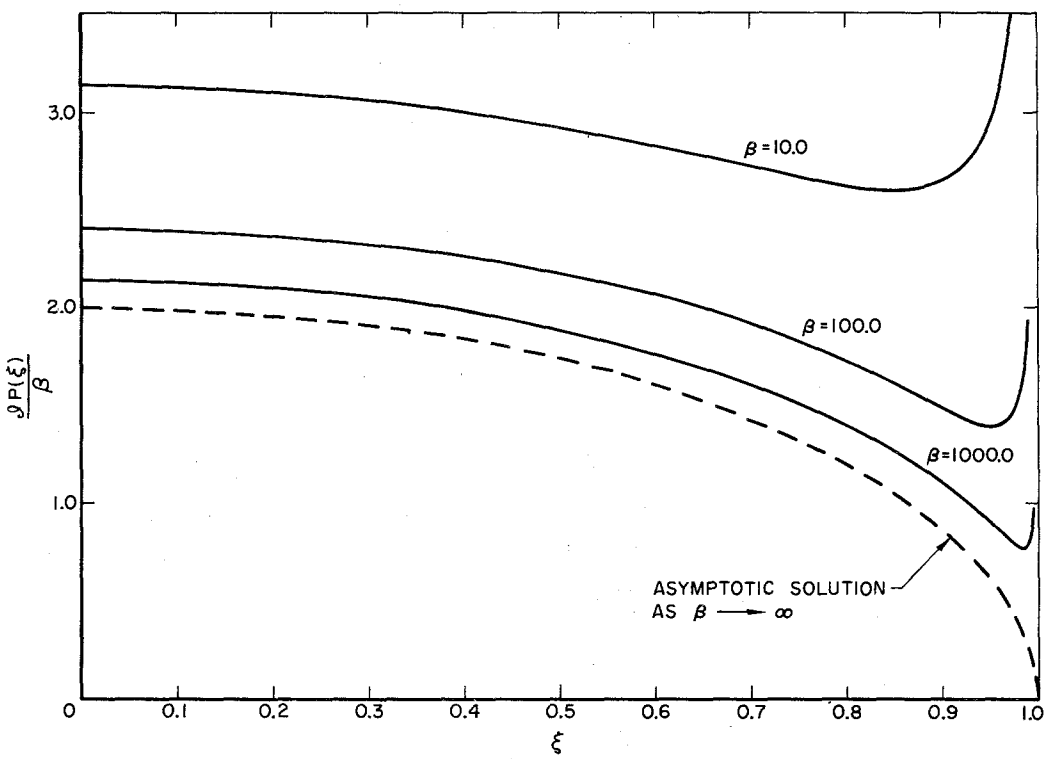

Figure 4. Pressure jump $\mathcal{I}P(\xi)$ across the ribbon in phase with acceleration. Computations for high frequencies $\beta = 10.0$ to $\beta = 1000.0$, scaled with respect to β.

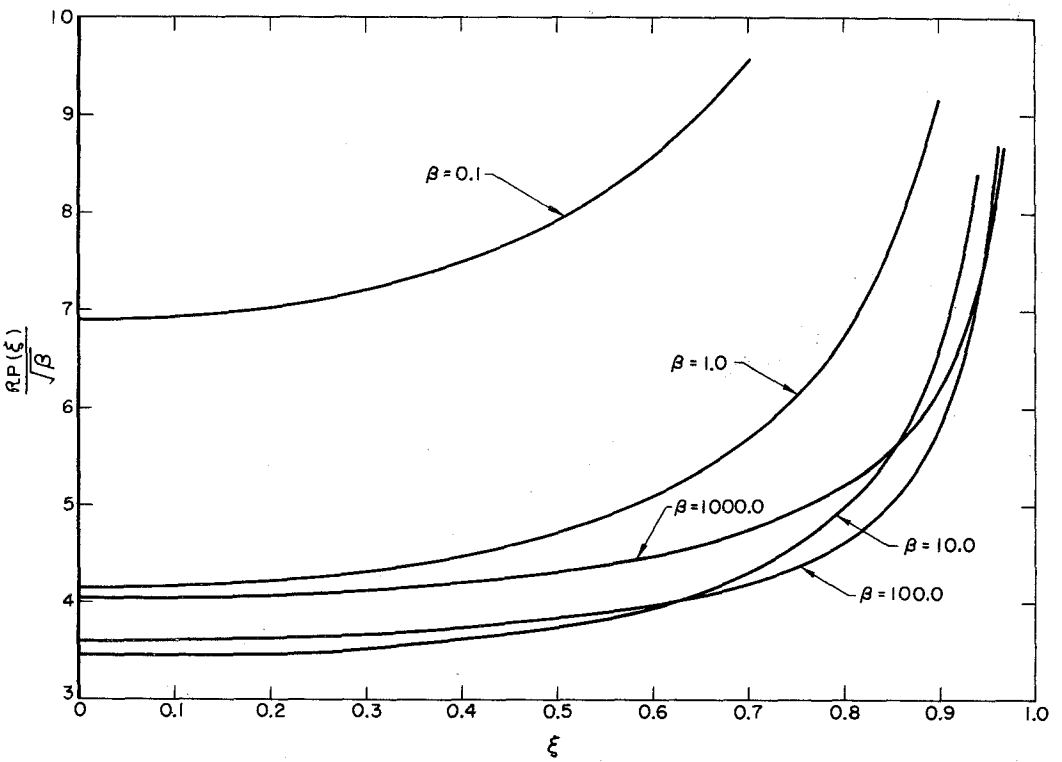

Figure 5. Pressure jump $\mathcal{R}P(\xi)$ across the ribbon in phase with velocity. Computations for $\beta = 0.1$ to $\beta = 1000.0$, scaled with respect to $\sqrt{\beta}$.

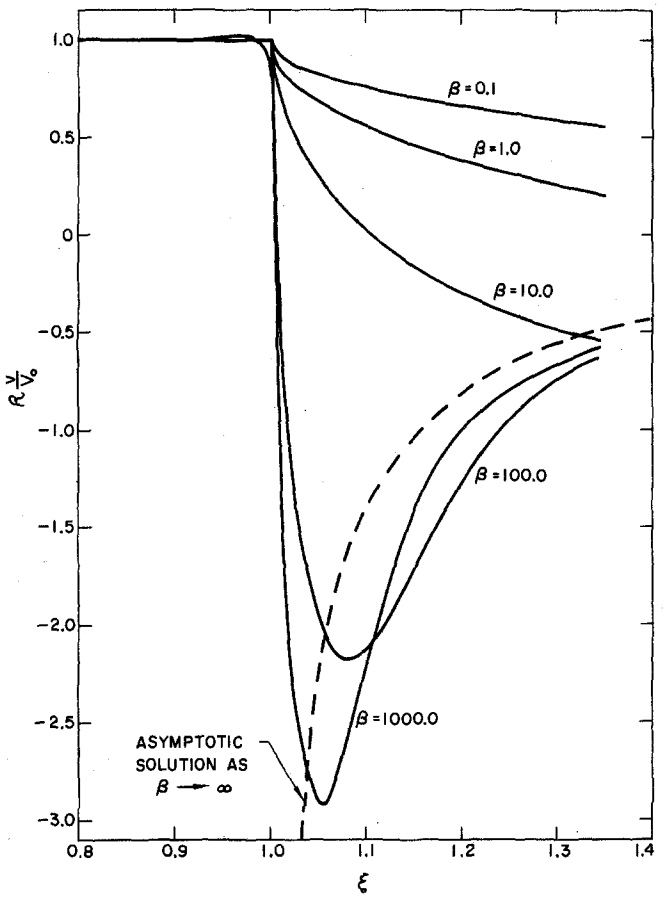

Figure 6. Vertical fluid velocity component $\mathcal{R}v(a\xi, 0)/V_0$ in phase with the velocity of the ribbon. The "smoothed-off" behavior shown for $\xi < 1$ is significant only for $\beta = 1000.0$, on the scale of this figure, and is to be interpreted as numerical inaccuracy.

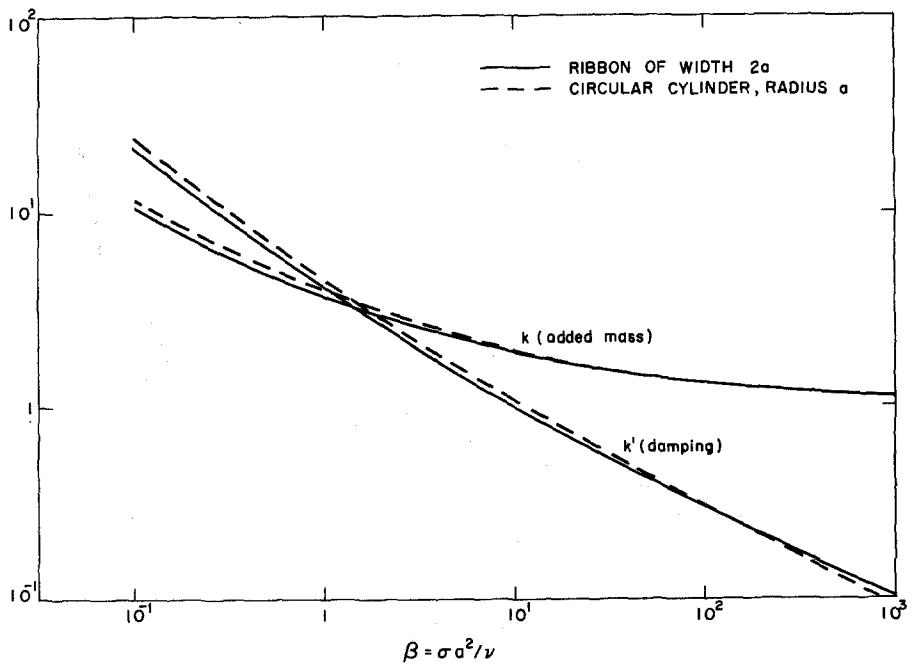

Figure 7. Force coefficients for oscillating cylinders. The force per unit length required to move a cylinder of width $2a$ with velocity $V_0 e^{i\sigma t}$ is $(k - ik') \cdot \rho\pi a^2 \cdot i\sigma V_0 e^{i\sigma t}$. The coefficients k, k' are given for circular cylinders and ribbons as functions of non-dimensional frequency $\beta = \sigma a^2/\nu$.

continuously but with negative infinite slope for all $\beta < \infty$. Again, we observe that the limit $\beta \to \infty$ is non-uniform near $\xi = 1.0$, as the limiting potential flow eq. (A1.10), shown dashed) has a negative infinite velocity at the sharp edge, $\xi \downarrow 1.0$. For larger ξ, the computed results at $\beta = 100.0$ and $\beta = 1000.0$ are quite close to the potential flow, whereas the lower frequency cases are beginning to look more like the singular Stokes limit (A1.7) as $\beta \to 0$, in which $v \sim -\log \xi$ as $\xi \to \infty$. The computed results for the imaginary part of v are not shown, but behave in a similar manner.

Finally, integration of $P(\xi)$ as in eq. (6.8) gives the force coefficients k, k' defined by eq. (4.8), which are plotted in Fig. 7 against β. A logarithmic scale is used for both abscissa and ordinate. Note that k is tending to unity and k' to zero like $C/\beta^{\frac{1}{2}}$ as $\beta \to \infty$, for some constant $C \sim 3.2$. Also shown as dashed curves are the corresponding results for a circular cylinder, calculated from Stokes' expression (4.10). It is remarkable how close the values are for the two differently-shaped cylinders over the whole four decades of frequency, from very slow oscillations adequately described by the steady Stokes equations all the way up to rapid oscillations of a predominantly inviscid nature. The difference between the dashed and solid curves is never more than 15% in this frequency range. For instance, at high frequency the limiting circle result for k' is $2\sqrt{2}/\beta^{\frac{1}{2}}$, about 13% lower than the computer estimate for the ribbon.

8. Concluding Remarks

Although the only numerical calculations presented here concern a very special oscillation of a special ribbon-like cylinder, there is no reason in principle why the integral equations derived for more general situations could not be solved in a similar manner. The most direct extension would be to solve first for more general modes of motion, while retaining the straight ribbon geometry. In a sense we have treated the worst possible case here, for if the ribbon moves in either of the two other directions we should have less cause to doubt linearization (no cause at all for axial oscillations!).

The straight ribbon has the advantages that first of all the integral equations for normal and tangential flow are de-coupled, and secondly that the simple frequency-uniformization used here works. It should be noted that these advantages of this particular geometry could be exploited in numerical solutions to other physical problems, e.g., in elastodynamic, electromagnetic or acoustic diffraction and radiation. The fact that the viscous flow problem for more general geometries requires solution of a pair of coupled integral equations is not in itself a great limitation, merely doubling the order of matrix to be inverted for a given accuracy, but the inability to render the solution even approximately uniformly valid with respect to frequency is disturbing. In the present viscous oscillation case, where the argument of the kernel is decaying exponentially as well as oscillating rapidly, this may not matter too much, but it would be a crucial point in any numerical solution to a diffraction problem.

Problems where the body is not necessarily rigid, in which the velocity on its instantaneous surface is a given function of position, are of great interest in connection with swimming motions of fish and small organisms (see e.g. Tuck 1968), and even perhaps in connection with boundary-layer stabilization by pliable surfaces. One mathematical peculiarity of such motions, which could have application to swimming, is that although the pressure jump must be unbounded at the ends of a ribbon in rigid-body oscillation, it will always be possible to combine a rigid translation with a suitable bending mode in such a way as to cancel the square-root singularity. In any swimming mode of a ribbon-like organism, it would seem likely that nature would prefer this to be the case. Since the numerical solution proceeds with no extra difficulty when the righthand side of the integral equation is a general function of position rather than a constant, there would seem plenty of scope for further numerical analysis of this problem.

The application of the present results to estimation of the effect of bilge keels and similar roll-damping devices on ships is minimal, and really we have no right to expect anything else. A quick glance at experimental measurements of the bilge-keel damping effect, e.g. Landweber and Thews 1938, shows that the phenomenon is non-linear. Presumably the main effect of such

drag-producing fins comes from vortex shedding at their sharp tips during the portion of the cycle at which the tips are moving most rapidly. We might have some hope for a quasi-steady inviscid vortex theory of such a flow, the principal characteristic of which would be a *quadratic* dependence of the damping force on the instantaneous rolling velocity.

However, it is of interest to consider how much a keel would add to the linear part of the damping, even though this can be significant only for very low amplitudes of roll. It is easy to see that we can increase the skin-friction part of the linear damping significantly with quite small keels. For instance, at frequencies high enough for the boundary layer thickness $\sqrt{\nu/\sigma}$ to be small compared with the radius of curvature R of a section, the skin-friction part of the drag on a rolling cylinder can be calculated from the classical Rayleigh solution (e.g. Landau and Lifschitz 1959, p. 90) for a flat plate, which gives for the tangential stress in phase with the velocity,

$$\frac{1}{\sqrt{2}} \cdot \rho\sqrt{\nu\sigma} \cdot \text{(instantaneous tangential velocity)}.$$

Hence if a clean circular cylinder of radius R, length L, is rotating with oscillatory angular velocity $\dot{\theta}$, the linear moment resisting it is

$$M_{\text{circle}} = \frac{1}{\sqrt{2}} \rho\sqrt{\nu\sigma} \cdot 2\pi RL \cdot R^2 \dot{\theta}$$

$$\sim 4.3\rho\sqrt{\nu\sigma}\, R^3 L\dot{\theta}\,. \tag{8.1}$$

Suppose now we attach a fin of width $2a$ to the cylinder. Then, using our computer estimate $k' = 3.2/\sqrt{\beta}$ for the damping force on the fin and neglecting interaction with the circle, we find an additional contribution to the damping moment of

$$M_{\text{fin}} = 3.2\ \rho\sqrt{\nu\sigma} \cdot \pi aL \cdot (\mathrm{R}+a)^2 \dot{\theta}$$

$$\sim 10.1 \frac{a}{R}\left(1 + \frac{a}{R}\right)^2 \cdot \rho\sqrt{\nu\sigma}\, R^3 L\dot{\theta}\,. \tag{8.2}$$

i.e. $M_{\text{fin}}/M_{\text{circle}} \sim 2.3 \dfrac{a}{R}\left(1 + \dfrac{a}{R}\right)^2$. Thus at $a/R = 0.1$, corresponding to a keel width only $\frac{1}{5}$ of the radius of the cylinder, we can more than double the linear viscous drag by adding four symmetrically located keels. This is not enough, of course, to explain the efficacy of bilge keels in practice, which is a non-linear phenomenon as discussed above, but could be important as a scale effect if rolling tests were made on models which were too small. Skin friction is not the only linear damping mechanism on sections without keels, and is in fact negligible at full scale, relative to wave damping. On the other hand, for small models of 1–2 feet beam, viscous and surface tension effects can dominate (see Vossers 1962 p. 57), and the predicted increase in the linear viscous part of the damping when bilge keels are fitted could be significant.

Appendix I

High and Low Frequency Asymptotes

In this appendix we consider in a heuristic manner the limiting forms of the integral equation (6.1) as $\beta \to 0$ and as $\beta \to \infty$. In viewing the results of this analysis one should bear in mind the corresponding limits of the boundary-value problem, respectively quasi-steady Stokes' flow as $\beta \to 0$, and inviscid potential flow as $\beta \to \infty$.

Substituting the small-argument expansion (5.8) of the kernel into the integral equation (6.1), we have

$$\int_{-1}^{1} P(\xi)[\log|\xi - \xi'| + C_1]\, d\xi = -4\pi\,, \tag{A1.1}$$

where

$$C_1 = \log \sqrt{i\beta} + \gamma + \frac{1}{2} - \log 2 \tag{A1.2}$$

is a constant. On differentiation of (A1.1) with respect to ξ', there results the homogeneous singular integral equation

$$\int_{-1}^{1} \frac{P(\xi)d\xi}{\xi - \xi'} = 0\,, \tag{A1.3}$$

which has a solution (Tricomi 1957, p. 174)

$$P(\xi) = \frac{C_2}{\sqrt{1-\xi^2}} \tag{A1.4}$$

for any constant C_2. But this is a solution of (A1.1) only for a particular value of C_2,

$$\begin{aligned} C_2 &= -4\pi \Big/ \left(\int_{-1}^{1} \frac{d\xi}{\sqrt{1-\xi^2}} \left[\log |\xi - \xi'| + C_1 \right] \right) \\ &= 4/(\log 2 - C_1) \\ &= 4/(0.309 - \log \sqrt{i\beta})\,. \end{aligned} \tag{A1.5}$$

Other quantities of interest can be written directly in terms of this constant C_2, e.g. the force on the ribbon is just

$$F_y = -\pi \frac{\mu V_0}{a} C_2\,, \tag{A1.6}$$

and the velocity across the x-axis is

$$v(a\xi, 0)/V_0 = \begin{cases} 1\,, & |\xi| < 1 \\ 1 + \dfrac{C_2}{4\pi} \log \left(|\xi| - \sqrt{\xi^2 - 1} \right), & |\xi| > 1\,. \end{cases} \tag{A1.7}$$

Note the manifestation of Stokes' paradox, in that this limiting solution does not satisfy the boundary condition at infinity.

More generally, with s instead of $i\sigma$, results such as (A1.5–A1.6) show that the $\mathscr{L}$-transform of the force on the ribbon behaves like $(\log s)^{-1}$ times the $\mathscr{L}$-transform (here unity) of the given velocity of translation. This is used in the text to estimate rates of decay of transients. It should be noted that such behavior is not confined to ribbons of zero thickness. The classical result (4.10) of Stokes on oscillating circular cylinders also has inverse logarithmic behavior as $\beta \to 0$, and it is no doubt possible to prove that this is a characteristic of the unsteady Stokes' equation, for any cylinder cross-section.

The high frequency limit $\beta \to \infty$ is apparently more singular, since the kernel resulting from use of the first term in the expansion (5.9) is not integrable. However, since we expect a solution satisfying $P(\pm 1) = 0$ in this limit (from consideration of the limiting boundary-value problem) we can integrate by parts, yielding a singular integro-differential equation

$$\int_{-1}^{1} \frac{P'(\xi)d\xi}{\xi - \xi'} = -2\pi i\beta\,, \tag{A1.8}$$

which has the bounded solution

$$P(\xi) = 2i\beta \sqrt{1-\xi^2}\,. \tag{A1.9}$$

This is a singular limit near $\xi = \pm 1$, since $P(\xi)/\beta$ is unbounded there for all $\beta < \infty$.

Although the above is hardly a rigorous derivation, the result (A1.9) is exactly what we would

find by solving the limiting boundary-value problem, corresponding to potential flow normal to the ribbon. The force is in phase with the acceleration, so that there is no damping, and the added mass is equal to that of the circumscribing circular cylinder. In order to find a non-zero damping we should have to carry the large β expansion further, e.g. by the Wiener–Hopf technique, in the manner of Carrier (Gortler and Tollmein 1955, p. 13) and Levine (1957). Direct boundary-layer methods, as in the method proposed by Segel (1960) do not seem to work for cylinders with sharp edges. From the boundary-layer nature of the large β approximation we can infer without actual performing this expansion that $\mathscr{R}P(\xi)=O(\sqrt{\beta})$, and hence that $k'\to C/\beta^{\frac{1}{2}}$ for some constant C. The trend of the computed results (Fig. 7) for large β would suggest $C\sim 3.2$ as compared with $2\sqrt{2}\sim 2.8$ for Stokes' circular cylinder result.

The velocity distribution on the x-axis is easily obtained either from (6.9) or from the limiting potential flow, in the form:

$$v(a\xi,0)/V_0=\begin{cases}1\,, & |\xi|<1\\ 1-|\xi|/\sqrt{\xi^2-1}\,, & |\xi|>1\,.\end{cases} \tag{A1.10}$$

This limiting velocity distribution is singular as $\xi\downarrow 1$, although v is continuous for all $\beta<\infty$. On the other hand, in contrast to the limit $\beta\to 0$, this limit does satisfy the boundary condition at ∞, since $v=O(\xi^{-1})$ as $\xi\to\infty$. Note also that this velocity is real, i.e. entirely in phase with the imposed velocity of the ribbon.

REFERENCES

Abramowitz, M. and Stegun, L. A. (eds.): *Handbook of Mathematical Functions.* National Bureau of Standards, Applied Mathematics Series No. 55, Washington, D.C., 1964.

Davis, P. J. and Rabinowitz, P.: Ignoring the singularity in approximate integration: *S.I.A.M. Jour. on Numerical Analysis* 2, pp. 367–383, 1965.

Gortler, H. and Tollmien, W. (eds.): 50 *Jahre Grenzschichtforschung*, Friedrich Vieweg, Braunschweig, 1955.

Landau, L. F. and Lifshitz, E. M.: Fluid Mechanics, Vol. 6 of *Course of Theoretical Physics*, Pergamon, Oxford 1959.

Levine, H.: Skin friction on a strip of finite width moving parallel to its length. *Jour. of Fluid Mechanics* 3, pp. 145–158, 1957.

Muskhelishvili, N. E.: *Singular Integral Equations*, Noordhoff, Groningen, 1953.

Rosenhead, L. (ed.): *Laminar Boundary Layers*, Oxford Univ. Press, 1963.

Segel, L. A.: A uniformly-valid asymptotic expansion of the solution to an unsteady boundary-layer problem. *Jour. of Mathematics and Physics* 39, pp. 189–197, 1960.

Thews, J. G. and Landweber, L.: The effect of the turn of the bilge on roll damping, *U.S. Experimental Model Basin Report No.* 442, Jan. 1938. Nav. Ship Res. and Dev. Center, Washington, D.C.

Tricomi, F. G.: *Integral Equations*, Interscience, New York, 1957.

Tuck, E. O.: A note on a swimming problem. *Jour. of Fluid Mechanics*, 31, pp. 305–308, 1968.

Vossers, G.: *Behavior of Ships in Waves.* Part IIC of Ships and Marine Engines, H. Stam, Haarlem, 1962.